Macrocycles Containing Tin. Crystal Structures and Molecular Mechanics Calculated Structures of Macrobicyclic Lewis Acidic Hosts

John H. Horner,[*] Phillip J. Squatritto,[†] Nancy McGuire, Joseph P. Riebenspies, and Martin Newcomb[*]

Department of Chemistry, Texas A&M University, College Station, Texas 77843

Received October 19, 1990

MM2 molecular modeling was employed in an analysis of the structures of several symmetrical macrobicycles containing tin atoms at the bridgehead positions. Compounds studied were 1,7-dichloro-1,7-distannabicyclo[5.5.5]heptadecane (**1a**) and the corresponding 1,7-diphenyl analogue (**2a**), 1,8-dichloro-1,8-distannabicyclo[6.6.6]eicosane (**1b**), 1,9-dichloro-1,9-distannabicyclo[7.7.7]tricosane (**1c**), 1,10-dichloro-1,10-distannabicyclo[8.8.8]hexacosane (**1d**) and the corresponding 1,10-diphenyl analogue (**2d**), 1,11-dichloro-1,11-distannabicyclo[9.9.9]nonacosane (**1e**), and 1,12-dichloro-1,12-distannabicyclo[10.10.10]dotriacontane (**1f**) and the corresponding 1,12-diphenyl analogue (**2f**). MM2 minimized structures generally closely reproduced the observed crystal structures when the crystal structure coordinates were used as the initial structures for minimizations. Alternative structures were also modeled, and the total energies of several possible structures were compared. The macrobicycles fall into one of two homologous series of structures, depending upon whether the connecting polymethylene chains have an odd or even number of carbon atoms. The odd-chain-length series typically have a low-energy structure of C_3 symmetry with the axis passing through the two tin atoms and the three chains in parallel conformations. For the even-chain-length series, an analogous series of structures with C_3 symmetry was found to be higher in energy than the typically observed C_2 symmetry containing two chains with antiparallel conformations and an axis passing through the center of the third chain. Crystal structures are reported for compounds **1a,c,e,f** and **2a,d,f**. Compound **1a** ($C_{15}H_{30}Sn_2Cl_2$) crystallized in the hexagonal space group $P6_3/m$ with a = 8.348 (2) Å, c = 16.672 (2) Å, V = 1006.1 (4) Å^3, and Z = 2. Compound **1c** ($C_{21}H_{42}Sn_2Cl_2$) crystallized in the monoclinic space group $P2_1/n$ with a = 12.482 (5) Å, b = 22.738 (2) Å, c = 9.196 (2) Å, β = 90.59 (2)°, V = 2610 (1) Å^3, and Z = 4. Compound **1e** ($C_{27}H_{54}Sn_2Cl_2$) crystallized in the monoclinic space group $C2/c$ with a = 24.476 (3) Å, b = 9.127 (2) Å, c = 14.283 (2), β = 90.80 (2)°, V = 3189 (3) Å^3, and Z = 4. Compound **1f** ($C_{30}H_{60}Sn_2Cl_2$) crystallized in the monoclinic space group $P2_1/c$ with a = 14.391 (3) Å, b = 17.080 (7) Å, c = 15.130 (3) Å, β = 106.76 (1)°, V = 3561 (2) Å^3, and Z = 4. Compound **2a** ($C_{27}H_{40}Sn_2$) crystallized in the monoclinic space group $P2_1/c$ with a = 16.645 (3) Å, b = 8.210 (4) Å, c = 19.331 (4) Å, β = 91.84 (2)°, V = 2640 (1) Å^3, and Z = 4. Compound **2d** ($C_{36}H_{58}Sn_2$) crystallized in the monoclinic space group $C2/c$ with a = 25.504 (7) Å, b = 9.112 (2) Å, c = 18.502 (4) Å, β = 124.14 (2)°, V = 3558.7 (15) Å^3, and Z = 4. Compound **2f** ($C_{42}H_{70}Sn_2$) crystallized in the monoclinic space group $C2/c$ with a = 25.947 (9) Å, b = 9.189 (3) Å, c = 21.256 (7) Å, β = 122.33 (2)°, V = 4262 (2) Å^3, and Z = 4.

Host–guest chemistry is now a sophisticated area of study. Anion binding by preorganized hosts, while not as extensively developed as cation binding, has progressed substantially in recent years. In aqueous media, anion binding has focused on polyammonium ion containing hosts.[1,2] Anion complexation in organic media usually has involved preorganized hosts containing multiple Lewis acidic binding sites.[3] Our group has explored anion complexation by macrocyclic and more complex hosts containing Lewis acidic tin atoms.[4]

As an aid for understanding the conformational energies of the tin-containing hosts, we wished to apply molecular mechanics modeling with the popular MM2 program.[5] Molecular mechanics modeling has been used for many years to provide insight into the conformational energies of carbocyclic macrocycles, crown ethers, cryptands, and other macrocyclic hosts.[6] Recent advances in the use of molecular dynamics methods suggest that even relatively unconstrained macrocycles with numerous possible conformations can be evaluated by modeling methods.[7]

In order to model our hosts, we developed a set of force field parameters for tetrahedral tin for use in MM2 modeling calculations and applied them in calculations of the structures of a number of simple stannanes.[8] In this work, we report the application of MM2 modeling for the

---

[†] Current address: Department of Chemistry, Central Michigan University, Mt. Pleasant, Michigan 48859.

(1) Reviews: (a) Schmidtchen, F. P. *Top. Curr. Chem.* **1986**, *136*, 101. (b) Dietrich, B. In *Inclusion Compounds*; Atwood, J. L., Davies, J. E. D. MacNicol, D. D., Eds.; Academic: London, 1984; Vol. 2, p 337. (c) Franke, J.; Voegtle, F. *Top. Curr. Chem.* **1986**, *132*, 135.

(2) For recent leading references, see the following: Hosseini, M. W.; Blacker, A. J.; Lehn, J.-M. *J. Am. Chem. Soc.* **1990**, *112*, 3896. Gleich, A.; Schmidtchen, F. P. *Chem. Ber.* **1990**, *123*, 907. Gleich, A.; Schmidtchen, F. P.; Mikulcik, P.; Müller, G. *J. Chem. Soc., Chem. Commun.* **1990**, *55*, Vögtle, F.; Wallon, A.; Müller, W. M.; Werner, U.; Nieger, M. *J. Chem. Soc., Chem. Commun.* **1990**, 158. Kurzmeier, H.; Schmidtchen, F. P. *J. Org. Chem.* **1990**, *55*, 3749. Tanaka, Y.; Kato, Y.; Aoyama, Y. *J. Am. Chem. Soc.* **1990**, *112*, 2807. Dietrich, B.; Lehn, J.-M.; Guilhem, J.; Pascard, C. *Tetrahedron Lett.* **1989**, *30*, 4125. Schneider, H.-J.; Kramer, R.; Simova, S.; Schneider, U. *J. Am. Chem. Soc.* **1988**, *110*, 6442. Fujita, T.; Lehn, J.-M. *Tetrahedron Lett.* **1988**, *29*, 1709. Tsukube, H. *J. Chem. Soc., Perkin Trans. 1* **1985**, 615. Gelb, R. I.; Lee, B. T.; Zompa, L. J. *J. Am. Chem. Soc.* **1985**, *107*, 909.

(3) For recent leading references, see the following: Galeffi, B.; Simard, M.; Wuest, J. D. *Inorg. Chem.* **1990**, *29*, 955. Nadeau, F.; Simard, M.; Wuest, J. D. *Organometallics* **1990**, *9*, 1311. Jurkschat, K.; Ruhlemann, A.; Tzschach, A. *J. Organomet. Chem.* **1990**, *381*, C53. Jurkschat, K.; Kuivila, H. G.; Liu, S. C.; Zubieta, J. A. *Organometallics* **1989**, *8*, 2755. Katz, H. E. *J. Org. Chem.* **1989**, *54*, 2179. Jung, M. E.; Xia, H. *Tetrahedron Lett.* **1988**, *29*, 297. Katz, H. E. *Organometallics* **1987**, *6*, 1134. Wuest, J. D.; Zacharie, B. *J. Am. Chem. Soc.* **1987**, *109*, 4714. Austin, M.; Gebreyes, K.; Kuivila, H. G.; Swami, K.; Zubieta, J. A. *Organometallics* **1987**, *6*, 834. Gielen, M.; Jurkschat, K.; Mahieu, B.; Apers, D. *J. Organomet. Chem.* **1985**, *286*, 145.

0276-7333/91/2310-1741$02.50/0

Table I. Summary of X-ray Diffraction Data for 1a,c,e and 2a[a]

	1a	1c	1e	2a
formula	$C_{15}H_{30}Sn_2Cl_2$	$C_{21}H_{42}Sn_2Cl_2$	$C_{27}H_{54}Sn_2Cl_2$	$C_{27}H_{40}Sn_2$
mol wt	518.69	602.85	687.01	601.99
cryst syst	hexagonal	monoclinic	monoclinic	monoclinic
a, Å	8.348 (2)	12.482 (5)	24.47 (3)	16.645 (3)
b, Å		22.738 (2)	9.127 (2)	8.210 (4)
c, Å	16.672 (2)	9.196 (2)	14.283 (2)	19.331 (4)
β, deg		90.59 (2)	90.80 (3)	91.84 (2)
V, Å^3	1006.1 (4)	2610 (1)	3189 (3)	2640 (1)
space group	$P6_3/m$ (No. 176)	$P2_1(n$ (No. 14)	$C2/c$ (No. 15)	$P2_1/c$ (No. 14)
Z	2	4	4	4
density, g/cm^3	1.71	1.53	1.43	1.51
F(000)	508	1208	1400	1208
scan type	2θ–ω	ω	ω	ω
μ(Mo Kα), cm^{-1}	27.51	21.32	17.53	19.09
transmissn factor	no cor	0.818–1.0	0.89–1.0	0.827–1.0
decay cor	no	no	yes	no
scan speed, deg/min	8	16	4	8
2θ range, deg	2–50	2–50	2–50	2–50
no. of unique data	420	4578	2984	4644
no. of obsd data ($I > 3\sigma(I)$)	283	2684	1063	3151
no. of variables	31	226	141	262
R, R_w[b]	0.023, 0.030	0.041, 0.055	0.052, 0.056	0.030, 0.058
largest peak, e/Å^3	0.26	1.13	0.46	0.62
goodness of fit	0.87[c]	1.43	2.00	1.65

[a] Instrument: Rigaku AFC5R. [b] $R = (\sum||F_o| - |F_c||)(\sum|F_o|)^{-1}$; $R_w = (\sum w(|F_o| - |F_c|)^2/\sum w|F_o|^2)^{0.5}$. [c] The GOF increased to 1.05 for $p = 0.03$; see Experimental Section.

Table II. Fractional Coordinates and Isotropic Thermal Parameters for 1a

atom	*x*	*y*	*z*	*B*(eq), Å^2
Sn	0.6667	0.3333	0.07329 (4)	3.32 (3)
Cl	0.6667	0.3334	−0.0706 (2)	5.1 (1)
C(1)	0.374 (1)	0.182 (1)	0.0968 (3)	4.3 (3)
C(2)	0.313 (1)	0.233 (1)	0.1737 (3)	3.8 (3)
C(3)	0.361 (1)	0.167 (1)	0.2500	2.8 (3)

structures of the macrobicyclic hosts **1a–f** and the phenyl-substituted precursors **2a,d,f**.[9] We also report the crystal structures of **1a**, **1c**, **1e**, **1f**, **2a**, **2d**,[10] and **2f**. The structures of **1b,d** were reported previously.[4g]

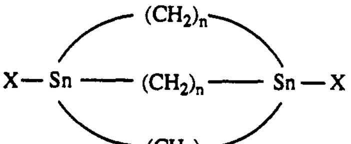

1: X = Cl
2: X = Ph

a: n = 5; b: n = 6; c: n = 7; d: n = 8; e: n = 9; f: n = 10

The initial goal of this work was to attempt to reproduce the experimental structures as closely as possible with MM2 modeling and then determine if there were predictive elements in the MM2 minimum energy structures. Bonding to the tin atoms was a primary concern, but it was apparent at the outset that the methylene chains in the hosts played an important role in the overall energies of the bicycles. For each structure, the modeling minimization was begun with the crystal structure coordinates. Other potential structures for the hosts were also used as initial points in modeling, especially in cases where the crystal structure was of low symmetry. It is unlikely that we could find global minimum energy conformations without the use of a molecular dynamics program and extensive minimization calculations,[7] but we believed that, for cases where an unusual host structure was found in the crystal, it was instructive to model alternative conformations that closely resembled those found for other hosts. In most of the cases, the minimum energy conformation found by MM2 modeling was also the relaxed molecular structure; i.e., the initial bond distances and angles of the crystal structure were altered only slightly to obtain the minimum energy structure. However, for some cases (**1c,e,f**), the MM2 minimum energy structure differed

---

(4) (a) Azuma, Y.; Newcomb, M. *Organometallics* **1984**, *3*, 9. (b) Newcomb, M.; Blanda, M. T.; Azuma, Y.; Delord, T. J. *J. Chem. Soc., Chem. Commun.* **1984**, 1159. (c) Newcomb, M.; Madonik, A. M.; Blanda, M. T.; Judice, J. K. *Organometallics* **1987**, *6*, 145. (d) Newcomb, M.; Horner, J. H.; Blanda, M. T. *J. Am. Chem. Soc.* **1987**, *109*, 7878. (e) Newcomb, M.; Blanda, M. T. *Tetrahedron Lett.* **1988**, *29*, 4261. (f) Blanda, M. T.; Horner, J. H.; Newcomb, M. *J. Org. Chem.* **1989**, *54*, 4626. (g) Newcomb, M.; Horner, J. H.; Blanda, M. T.; Squattrito, P. J. *J. Am. Chem. Soc.* **1989**, *111*, 6294. (h) Blanda, M. T.; Newcomb, M. *Tetrahedron Lett.* **1989**, *30*, 3501.

(5) Allinger, N. L. *J. Am. Chem. Soc.* **1977**, *99*, 8127.

(6) (a) Allinger, N. L.; Gorden, B.; Profeta, S., Jr. *Tetrahedron* **1980**, *36*, 859. (b) Bovill, M. J.; Chadwick, D. J.; Sutherland, I. O.; Watkin, D. *J. Chem. Soc., Perkin Trans. 2* **1980**, 1529. (c) Wipff, G.; Weiner, P.; Kollman, P. *J. Am. Chem. Soc.* **1982**, *104*, 3249. (d) Perrin, R.; Decoret, C.; Bertholon, G.; Lamartine, R. *Nouv. J. Chim.* **1983**, *7*, 263. (e) Dobler, M. *Chimia* **1984**, *38*, 415. (f) Drew, M. G. B.; Hollis, S.; Yates, P. C. *J. Chem. Soc., Dalton Trans.* **1985**, 1829. (g) Wipff, G.; Kollman, P. *Nouv. J. Chim.* **1985**, *9*, 458. (h) Kollman, P. A.; Wipff, G.; Singh, U. C. *J. Am. Chem. Soc.* **1985**, *107*, 2212. (i) Geue, R.; Jacobson, S. H.; Pizer, R. *J. Am. Chem. Soc.* **1986**, *108*, 1150. (j) Masek, B. B.; Santarsiero, B. D.; Dougherty, D. A. *J. Am. Chem. Soc.* **1987**, *109*, 4373. (k) Grootenhuis, P. D. J.; van Eerden, J.; Sudhölten, E. J. R.; Reinhoudt, D. N.; Roos, A.; Harkema, S.; Feil, D. *J. Am. Chem. Soc.* **1987**, *109*, 4792. (l) Uiterwijk, J. W. H. M.; Harkema, S.; Feil, D. *J. Chem. Soc., Perkin Trans. 2* **1987**, 721. (m) Damewood, J. R.; Anderson, W. P.; Urban, J. J. *J. Comput. Chem.* **1988**, *9*, 111. (n) Hancock, R. D. *Acc. Chem. Res.* **1990**, *23*, 253.

(7) (a) van Eerden, J.; Harkema, S.; Feil, D. *J. Phys. Chem.* **1988**, *92*, 5076. (b) Loncharich, R. J.; Seward, E.; Ferguson, S. B.; Brown, F. K.; Diederich, F.; Houk, K. N. *J. Org. Chem.* **1988**, *53*, 3479. (c) Billeter, M.; Howard, A. E.; Kuntz, I. D.; Kollman, P. A. *J. Am. Chem. Soc.* **1988**, *110*, 8385. (d) Mazor, M. H.; McCammon, J. A.; Lybrand, T. P. *J. Am. Chem. Soc.* **1989**, *111*, 55. (e) Gehin, D.; Wipff, G.; Kollman, P. A. *J. Am. Chem. Soc.* **1989**, *111*, 3011. (f) Grootenhuis, P. D. J.; Kollman, P. A. *J. Am. Chem. Soc.* **1989**, *111*, 4046. (g) Hase, W. L.; Richou, M.-C.; Mondro, S. L. *J. Phys. Chem.* **1989**, *93*, 539. (h) Straatsma, T. P.; McCammon, J. A. *J. Chem. Phys.* **1989**, *91*, 3631. (i) Wipff, G.; Wurtz, J.-M. *Nouv. J. Chim.* **1989**, *13*, 807. (j) Auffinger, P.; Wipff, G. *J. Comput. Chem.* **1990**, *11*, 19. (k) Dang, L. X.; Kollman, P. A. *J. Am. Chem. Soc.* **1990**, *112*, 5716. (l) Kollman, P. A.; Merz, K. M., Jr. *Acc. Chem. Res.* **1990**, *23*, 246.

(8) Horner, J. H.; Newcomb, M. *Organometallics*, preceding paper in this issue.

(9) For the preparation of these compounds, see ref 4f.

(10) The structure of **2d** reported earlier[4b] has been found to be in error; a corrected structure is reported here.

Table III. Fractional Coordinates and Isotropic Thermal Parameters for 2a

atom	*x*	*y*	*z*	*B*(eq), Å^2
Sn(1)	0.38762 (3)	0.15808 (6)	0.91889 (2)	4.80 (2)
Sn(2)	0.09660 (3)	0.15348 (5)	1.10754 (2)	4.30 (2)
C(1)	0.4373 (4)	0.222 (1)	1.0205 (4)	6.3 (4)
C(2)	0.3860 (4)	0.3118 (9)	1.0709 (4)	5.6 (4)
C(3)	0.3233 (4)	0.2081 (9)	1.1038 (3)	5.0 (3)
C(4)	0.2698 (4)	0.300 (1)	1.1514 (4)	5.6 (4)
C(5)	0.1996 (4)	0.198 (1)	1.1778 (3)	5.7 (4)
C(6)	0.3436 (4)	−0.086 (1)	0.9101 (4)	6.1 (4)
C(7)	0.3047 (4)	−0.1627 (8)	0.9738 (5)	6.4 (4)
C(8)	0.2220 (4)	−0.0968 (9)	0.9856 (4)	5.1 (3)
C(9)	0.1839 (5)	−0.1635 (8)	1.0509 (4)	6.0 (4)
C(10)	0.1009 (4)	−0.0906 (9)	1.0653 (4)	5.3 (3)
C(11)	0.3098 (4)	0.3340 (9)	0.8709 (4)	6.2 (4)
C(12)	0.2197 (4)	0.308 (1)	0.8781 (4)	5.7 (4)
C(13)	0.1900 (4)	0.3527 (8)	0.9486 (3)	4.9 (3)
C(14)	0.1014 (4)	0.3126 (8)	0.9584 (3)	5.1 (3)
C(15)	0.0734 (4)	0.3423 (8)	1.0315 (4)	5.2 (3)
C(16)	0.4904 (4)	0.1589 (8)	0.8533 (4)	5.0 (3)
C(17)	0.5561 (4)	0.2557 (9)	0.8667 (4)	5.1 (3)
C(18)	0.6197 (4)	0.258 (1)	0.8229 (4)	5.7 (4)
C(19)	0.6175 (4)	0.163 (1)	0.7648 (4)	5.9 (4)
C(20)	0.5527 (4)	0.069 (1)	0.7504 (4)	6.8 (4)
C(21)	0.4898 (4)	0.067 (1)	0.7933 (4)	6.4 (4)
C(22)	−0.0090 (4)	0.1610 (8)	1.1719 (3)	4.7 (3)
C(23)	−0.0771 (4)	0.249 (1)	1.1543 (3)	5.4 (4)
C(24)	−0.1439 (4)	0.256 (1)	1.1959 (4)	6.6 (4)
C(25)	−0.1421 (5)	0.173 (1)	1.2566 (4)	6.6 (4)
C(26)	−0.0745 (6)	0.086 (1)	1.2770 (5)	8.7 (6)
C(27)	−0.0070 (5)	0.081 (1)	1.2347 (4)	7.3 (5)

Table IV. Fractional Coordinates and Isotropic Thermal Parameters for 1c

atom	*x*	*y*	*z*	*B*(eq), Å^2
Sn(1)	0.20068 (6)	0.24734 (2)	0.03459 (7)	7.11 (4)
Sn(2)	0.25298 (4)	0.58531 (2)	−0.12799 (5)	5.71 (3)
Cl(1)	0.2364 (2)	0.1448 (1)	0.0548 (3)	8.7 (1)
Cl(2)	0.2456 (2)	0.6896 (1)	−0.1043 (3)	9.5 (2)
C(1)	0.3488 (8)	0.2774 (4)	−0.057 (1)	8.1 (5)
C(2)	0.3455 (7)	0.3346 (4)	−0.144 (1)	7.9 (5)
C(3)	0.4513 (7)	0.3518 (4)	−0.203 (1)	8.0 (5)
C(4)	0.4471 (7)	0.4059 (4)	−0.297 (1)	7.5 (5)
C(5)	0.4201 (7)	0.4622 (4)	−0.2185 (9)	6.9 (5)
C(6)	0.4215 (6)	0.5169 (4)	−0.3125 (9)	6.9 (5)
C(7)	0.4047 (6)	0.5737 (4)	−0.2325 (9)	6.7 (4)
C(8)	0.0559 (9)	0.2476 (4)	−0.093 (1)	9.8 (7)
C(9)	0.0441 (8)	0.2940 (5)	−0.208 (1)	9.9 (7)
C(10)	0.0520 (7)	0.3560 (4)	−0.152 (1)	7.7 (5)
C(11)	0.0546 (7)	0.4037 (5)	−0.269 (1)	8.2 (6)
C(12)	0.0810 (8)	0.4644 (4)	−0.210 (1)	8.1 (5)
C(13)	0.0891 (7)	0.5130 (5)	−0.314 (1)	8.1 (5)
C(14)	0.1090 (7)	0.5720 (4)	−0.251 (1)	7.9 (5)
C(15)	0.172 (1)	0.2692 (5)	0.258 (1)	11.2 (8)
C(16)	0.239 (1)	0.3131 (5)	0.328 (1)	9.9 (7)
C(17)	0.229 (1)	0.3735 (5)	0.271 (1)	14 (1)
C(18)	0.254 (1)	0.4208 (5)	0.335 (1)	14 (1)
C(19)	0.2482 (7)	0.4823 (4)	0.2928 (8)	6.4 (4)
C(20)	0.2556 (7)	0.4952 (4)	0.1333 (8)	6.9 (5)
C(21)	0.2483 (7)	0.5593 (4)	0.0943 (9)	6.8 (5)

greatly from the crystal structure even though the relaxed molecular structure represented a local minimum. In general, the most important energy factor in these cases was the interchain ver der Waals terms.

As noted in the accompanying work,[8] the results of the macrobicycle calculations were used to evaluate and refine the tin–chlorine force field parameters. For this purpose, only the relaxed molecular structures were used for comparisons even when these structures were not the minimum energy conformations found in MM2 modeling.

Results

In consideration of the structures of the macrobicyclic species 1 and 2, it is convenient to divide the compounds into two groups according to the chain lengths of the polymethylene linkers. In terms of general structural features, the odd-chain-length and even-chain-length bicycles comprise two homologous series.

Table V. Fractional Coordinates and Isotropic Thermal Parameters for 1e

atom	*x*	*y*	*z*	*B*(eq), Å^2
Sn(1)	0.81471 (4)	0.5621 (1)	0.42923 (7)	7.03 (6)
Cl(1)	0.7396 (2)	0.5014 (5)	0.5262 (3)	9.7 (3)
C(1)	0.8535 (7)	0.355 (2)	0.410 (1)	11 (1)
C(2)	0.8544 (9)	0.290 (2)	0.320 (1)	12 (1)
C(3)	0.902 (1)	0.181 (2)	0.299 (1)	15 (2)
C(4)	0.9523 (9)	0.260 (3)	0.270 (2)	15 (2)
C(5)	1.0000	0.185 (5)	0.2500	15 (3)
C(6)	0.7766 (5)	0.660 (2)	0.311 (1)	8 (1)
C(7)	0.8127 (6)	0.761 (2)	0.253 (1)	7.5 (9)
C(8)	0.8628 (6)	0.688 (2)	0.211 (1)	7.7 (9)
C(9)	0.9041 (6)	0.787 (1)	0.163 (1)	7.2 (8)
C(10)	0.9533 (6)	0.700 (2)	0.127 (1)	6.8 (8)
C(11)	0.9970 (6)	0.795 (2)	0.084 (1)	8 (1)
C(12)	1.0459 (6)	0.705 (2)	0.049 (1)	8 (1)
C(13)	1.0935 (7)	0.790 (2)	0.015 (1)	9 (1)
C(14)	0.8597 (6)	0.701 (2)	0.525 (1)	8 (1)

Table VI. Selected Interatomic Distances and Angles for 1a, 2a, 1c, and 1e

	Interatomic Distances (Å) in **1a**		
Sn–Sn	5.892 (2)	Sn–Cl	2.398 (3)
Sn–C(1)	2.152 (7)	C(1)–C(2)	1.518 (9)
C(2)–C(3)	1.519 (7)		
	Bond Angles (deg) in **1a**		
Cl–Sn–C(1)	100.5 (2)	C(1)–Sn–C(1)	116.8 (1)
Sn–C(1)–C(2)	115.7 (5)	C(1)–C(2)–C(3)	114.8 (5)
	Interatomic Distances (Å) in **2a**		
Sn(1)–Sn(2)	6.156 (1)	Sn(1)–C(1)	2.170 (7)
Sn(1)–C(6)	2.141 (8)	Sn(1)–C(11)	2.132 (8)
Sn(1)–C(16)	2.161 (6)	Sn(2)–C(5)	2.183 (7)
Sn(2)–C(10)	2.166 (7)	Sn(2)–C(15)	2.162 (7)
Sn(2)–C(22)	2.186 (6)		
	Bond Angles (deg) in **2a**		
C(16)–Sn(1)–C(1)	104.1 (3)	C(16)–Sn(1)–C(6)	103.6 (2)
C(16)–Sn(1)–C(11)	103.0 (3)	C(1)–Sn(1)–C(6)	114.4 (3)
C(1)–Sn(1)–C(11)	116.1 (3)	C(6)–Sn(1)–C(11)	113.7 (3)
C(22)–Sn(2)–C(5)	105.7 (3)	C(22)–Sn(2)–C(10)	106.1 (2)
C(22)–Sn(2)–C(15)	103.7 (2)	C(5)–Sn(2)–C(10)	110.7 (3)
C(5)–Sn(2)–C(15)	115.1 (3)	C(10)–Sn(2)–C(15)	114.5 (3)
	Interatomic Distances (Å) in **1c**		
Sn(1)–Sn(2)	7.857 (1)	Sn(1)–Cl(1)	2.381 (2)
Sn(2)–Cl(2)	2.383 (2)	Sn(1)–C(1)	2.15 (1)
Sn(1)–C(8)	2.15 (1)	Sn(1)–C(15)	2.15 (1)
Sn(2)–C(7)	2.149 (8)	Sn(2)–C(14)	2.136 (9)
Sn(2)–C(21)	2.129 (8)		
	Bond Angles (deg) in **1c**		
Cl(1)–Sn(1)–C(1)	100.4 (3)	Cl(1)–Sn(1)–C(8)	101.6 (3)
Cl(1)–Sn(1)–C(15)	100.7 (3)	C(1)–Sn(1)–C(8)	120.4 (4)
C(1)–Sn(1)–C(15)	117.1 (4)	C(8)–Sn(1)–C(15)	112.0 (5)
Cl(2)–Sn(2)–C(7)	101.4 (2)	Cl(2)–Sn(2)–C(14)	99.0 (3)
Cl(2)–Sn(2)–C(21)	100.8 (2)	C(7)–Sn(2)–C(14)	119.0 (3)
C(7)–Sn(2)–C(21)	115.3 (3)	C(14)–Sn(2)–C(21)	116.1 (3)
	Interatomic Distances (Å) in **1e**		
Sn(1)–Sn(1a)	10.48 (1)	Sn(1)–Cl(1)	2.382 (4)
Sn(1)–C(1)	2.13 (2)	Sn(1)–C(6)	2.12 (1)
Sn(1)–C(14)	2.15 (1)		
	Bond Angles (deg) in **1e**		
Cl(1)–Sn(1)–C(1)	102.5 (5)	Cl(1)–Sn(1)–C(6)	103.1 (4)
Cl(1)–Sn(1)–C(14)	99.2 (4)	C(1)–Sn(1)–C(6)	117.6 (6)
C(1)–Sn(1)–C(14)	112.2 (7)	C(6)–Sn(1)–C(14)	118.3 (6)

Odd-Chain-Length Bicycles. Crystal structures have been obtained for compounds **1a,c,e** and **2a**, in which the two tin atoms are linked by odd-chain-length methylene bridges. A summary of the diffraction data for these

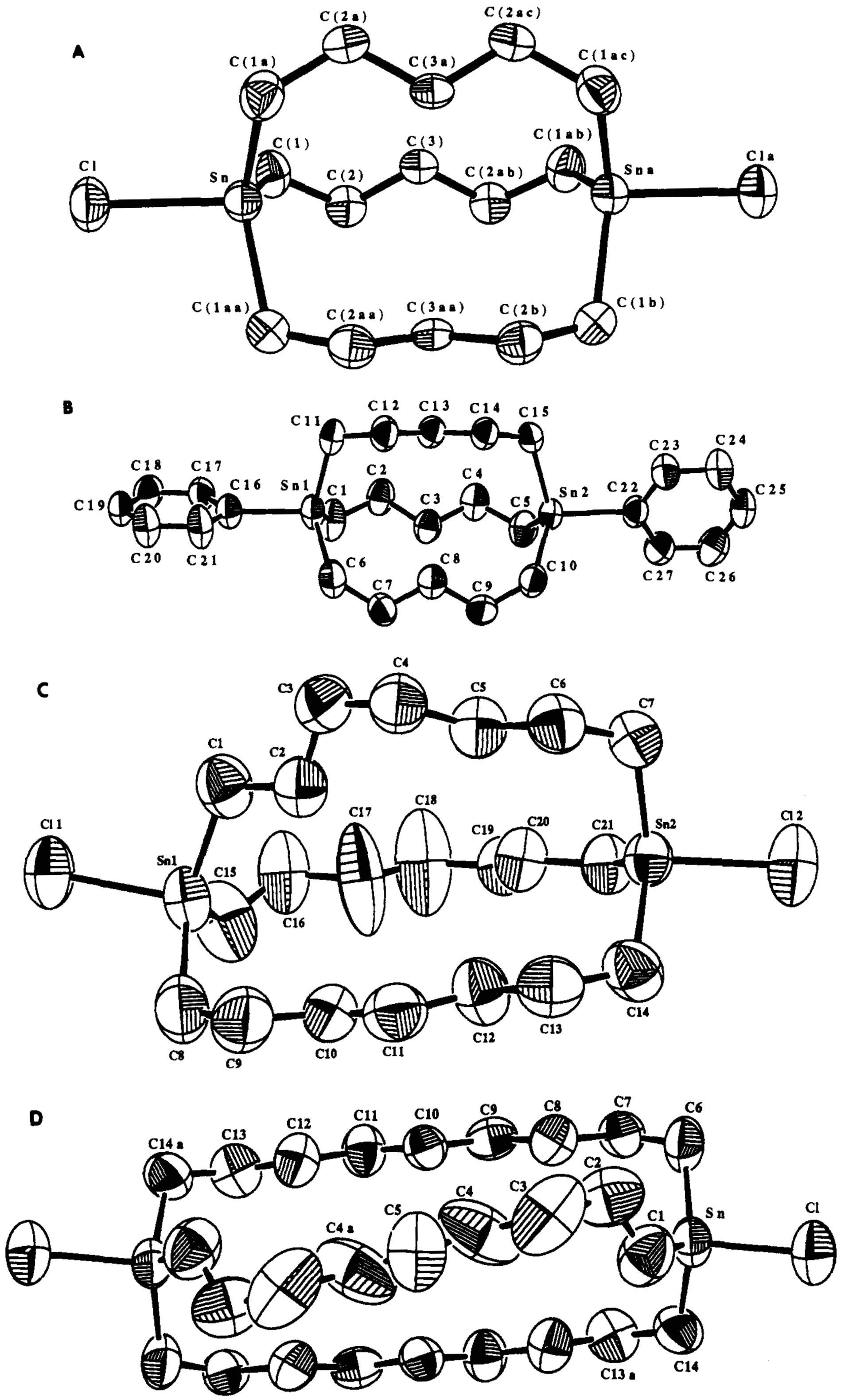

Figure 1. ORTEP drawings at 50% probability of the structures of **1a** (A), **2a** (B), **1c** (C), and **1e** (D).

compounds is given in Table I. Fractional coordinates are given in Tables II–V, and selected distances and angles are given in Table VI. ORTEP drawings of these four compounds are shown in Figure 1.

The C-5 bicycles (**1a** and **2a**) demonstrate the high-symmetry structural type possible with the odd-chain-length bicycles. Compound **1a** crystallized in the hexagonal crystal system with the 3-fold *c* crystallographic axis running lengthwise through the molecule. Thus, the three polymethylene chains in **1a** are equivalent. For the diphenyl precursor **2a**, a C_3 axis is precluded by the phenyl rings, but the methylene chains still adopt a conformation with local 3-fold symmetry, and thus, the structure of **2a** is quite similar to that of **1a**. Figure 2 shows views of **1a** and **2a** in which the 3-fold symmetry of the chains is apparent. For both **1a** and **2a**, as one moves down each chain, the dihedral angles are in a gauche–anti–anti–gauche (g–a_2–g) relationship.

MM2 calculations indicated that the g–a_2–g conformations of the methylene chains in **1a** and **2a** resulted in

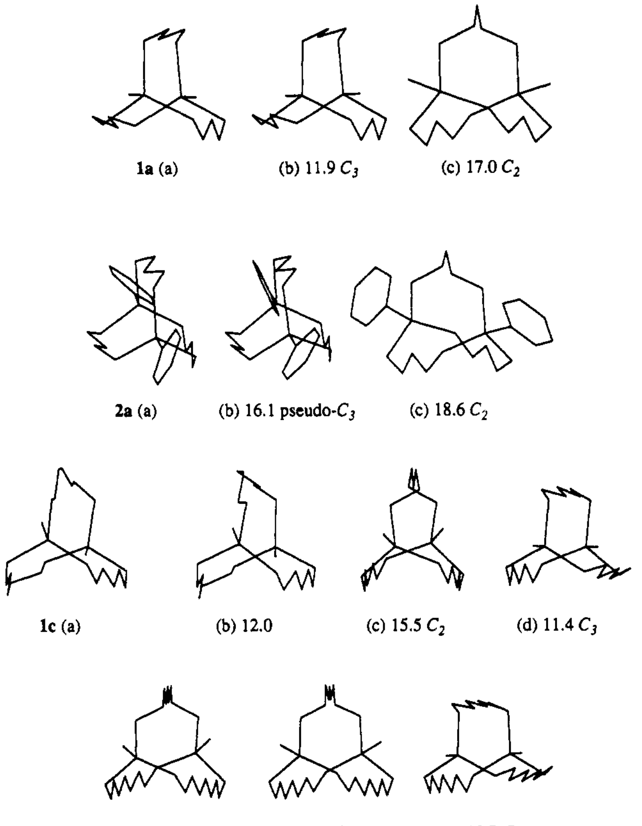

1a (a) (b) 11.9 C_3 (c) 17.0 C_2

2a (a) (b) 16.1 pseudo-C_3 (c) 18.6 C_2

1c (a) (b) 12.0 (c) 15.5 C_2 (d) 11.4 C_3

1e (a) (b) 14.9 C_2 (c) 10.7 C_3

Figure 2. Odd-chain-length macrobicycles. Structures a are X-ray structures. Other structures are MM2 minimized results; the total energies in kcal/mol of the structures and symmetry element, if present, are given under the structure. Structures b are MM2 minimized structures starting from the X-ray structure coordinates.

Table VII. Comparison of Experimental and Calculated Structures for 1a

	MM2	exptl[a]
Interatomic Distances (Å)		
Sn–Sn	5.926	5.892 (2)
Sn–Cl	2.380	2.398 (3)
Sn–C(1)	2.153	2.152 (7)
Bond Angles (deg)		
Cl–Sn–C(1)	100.6	100.5 (2)
Cl–Sn–C(1)	116.7	116.8 (1)
Sn–C(1)–C(2)	115.2	115.7 (5)
Torsion Angles (deg)		
Sn–C(1)–C(2)–C(3)	-75.9	-72.5 (7)
C(1)–C(2)–C(3)–C(2a)	173.3	175.2 (4)
Cl–Sn–C(1)–C(2)	-149.3	-149.8 (5)

[a] X-ray crystal structure, this work.

low-energy structures. Extensive minimization involving other conformations failed to locate any minima lower in energy. Table VII and Table XVI (supplementary material) contain summaries of the calculated and crystallographic structures. Figure 2 shows comparisons of the crystal structures and MM2 minimum-energy structures for **1a** and **2a**. In both cases, agreement between the MM2 calculated geometry and the crystal structure was remarkably good. For the calculated structures of **1a** and **2a**, the Sn–Sn distances, which reflect a summation of many interactions, differ from those in the crystal structures by 0.034 Å (0.5%) and 0.012 Å (0.2%), respectively. There is almost exact agreement between the calculated and experimental bond distances, bond angles, and torsion angles for **1a**. In the case of **2a**, the overall agreement is also very good; the average deviation of the calculated bond angles from the experimental values is 1.6° with the largest deviations (4.4°) involving one carbon atom, C(10), in the structure.

Table VIII. Comparison of Calculated and Experimental Structures for 1e

	MM2	exptl[a]
Interatomic Distances (Å)		
Sn–Sn	10.656	10.48 (1)
Sn–Cl	2.378	2.382 (4)
Sn–C(1)	2.148	2.13 (2)
Sn–C(6)	2.153	2.12 (1)
Sn–C(14)	2.151	2.15 (1)
Bond Angles (deg)		
Cl–Sn–C(1)	103.4	102.5 (5)
Cl–Sn–C(6)	104.1	103.1 (4)
Cl–Sn–C(14)	103.8	99.2 (4)
C(1)–Sn–C(6)	115.6	117.6 (6)
C(1)–Sn–C(14)	111.3	112.2 (7)
C(6)–Sn–C(14)	116.6	118.3 (6)
Sn–C(1)–C(2)	114.5	120 (1)
Sn–C(6)–C(7)	115.8	115.6 (9)
Sn–C(14)–C(13a)	115.3	118 (1)
Torsion Angles (deg)		
Sn–C(1)–C(2)–C(3)	153.9	155 (1)
Sn–C(6)–C(7)–C(8)	68.9	61 (1)

[a] X-ray crystal structure, this work.

It is likely that the relief of interchain van der Waals interactions is the major factor that determines the conformation of the methylene chains in **1a** and **2a**. The closest interchain H–H distance in the minimized structures is 2.20 Å, which is just beyond the van der Waals contact distance. During the minimization process, van der Waals interactions were seen to be a major factor in raising the calculated total MM2 energies of several alternative trial geometries.

The C-9 dichloro bicycle **1e** exemplifies a second structural type possible for the odd-chain-length bicycles. This molecule has a C_2 axis that is perpendicular to the tin–tin axis and runs through the central atom of one of the chains. The ORTEP drawing of **1e** (Figure 1) shows a view directly down the C_2 axis. In Figure 2, it can be seen that chain 2 (C(6) to C(14a)) and chain 3 (C(6a) to C(14)) are symmetry-equivalent; these chains adopt g–a_6–g conformation that serves to minimize the interchain van der Waals interactions. Chain 1 of **1e** (C(1) to C(1a)) has an a–g–a_4–g–a conformation that is expected to be somewhat higher in energy than the g–a_6–g alternative.

When the crystal structure coordinates of **1e** were used as the starting point in MM2 modeling, a minimum was quickly reached. The calculated and experimental features matched closely (Table VIII); for example, the calculated Sn–Sn distance of 10.66 Å was only 0.18 Å longer than the experimental distance. However, the C_2 symmetry structure of **1e** was not the minimum-energy structure found. In analogy to the C-5 bicycles **1a** and **2a**, a lower energy structure was found to be that with C_3 symmetry (Figure 2) wherein the three equivalent methylene chains each have a g–a_6–g conformation. The C_3 symmetry structure of **1e** was more than 4 kcal/mol lower in energy than the C_2 symmetry structure adopted by the molecule in the crystal. This energy difference results mainly from the occurrence of two gauche interactions within chain 1 rather than at the ends of the chain because the Sn–C–C–C torsion barrier is inconsequential in comparison to the C–C–C–C torsion barrier.[8] Apparently, intermolecular forces in the solid state compensate for an inherent preference for the C_3 symmetry structure over the C_2 symmetry structure.

Table IX. Summary of X-ray Diffraction Data for 1f, 2d, and 2f

	1f	**2d**	**2f**
formula	$C_{30}H_{60}Sn_2Cl_2$	$C_{36}H_{58}Sn_2$	$C_{42}H_{70}Sn_2$
mol wt	729.09	728.20	812.40
cryst syst	monoclinic	monoclinic	monoclinic
a, Å	14.391 (3)	25.504 (7)	25.947 (9)
b, Å	17.080 (7)	9.112 (2)	9.189 (3)
c, Å	15.130 (3)	18.502 (4)	21.156 (7)
β, deg	106.76 (1)	124.14 (2)	122.33 (2)
V, Å^3	3561 (2)	3558.7 (15)	4262 (2)
space group	$P2_1/c$ (No. 14)	$C2/c$ (No. 15)	$C2/c$ (No. 15)
Z	4	4	4
density, g/cm^3	1.36	1.359	1.27
F(000)	1496	1496	1688
instrument	Rigaku AFC5R	Nicolet R3m	Rigaku AFC5R
scan type	ω	ω–2θ	ω
μ(Mo Kα), cm^{-1}	15.74	14.29	11.99
transmissn factor	0.795–1.0	no cor	0.813–1.0
decay cor	yes	no	yes
scan speed, deg/min	8	1.5–14.65	4
2θ range, deg	2–50	4–50	2–45
no. of unique data	5256	3148	2452
no. of obsd data	1757[a]	1797[b]	939[c]
no. of variables	307	128	199
R, R_w[d]	0.086, 0.105	0.0787, 0.0806	0.062, 0.064
largest peak, e/Å^3	0.96	0.79	0.52
goodness of fit	2.46	6.14	1.47

[a] $I > 3\sigma(I)$. [b] $F > 4\sigma(F)$. [c] $I > 2\sigma(I)$. [d] $R = (\sum||F_o| - |F_c||)(\sum|F_o|)^{-1}$; $R_w = (\sum w(|f_o| - |F_c|)^2/\sum w|F_o|^2)^{0.5}$.

The C-7 bicycle **1c** adopts neither of the high-symmetry structures discussed above, but a portion of the structure is similar to both (Figures 1 and 2). One of the chains in **1c**, C(8) to C(14), has the highly regular g–a$_4$–g conformation similar to the chains in **1e**, and another chain, C(1) to C(7), has only one carbon atom, C(2), out of place for the g–a$_{n-3}$–g conformation. The third chain of **1c**, C(15) to C(21), is highly irregular, and the large thermal parameters for C(15), C(17), and C(18) (Figure 1) indicate serious disorder for this chain in the crystal. In view of the high symmetry present in the crystal structures of other members of this series of compounds, the crystal structure of **1c** was examined carefully; the lack of symmetry is real.

With the crystal structure coordinates of **1c** as the starting point, an MM2 minimum was quickly reached for the relaxed molecular structure. With the exception of the disordered chain, C(15) to C(21), the calculated distances and angles closely matched those of the crystal structure (Table XVII, supplementary material). Figure 2 shows comparisons of the crystal structure and the MM2 minimized structures.

In the MM2 minimization of **1c**, the poor torsion angles involving the disordered chain in the crystal rotated to reduce unfavorable interactions. This behavior prompted an examination of alternative structures for **1c** in some detail. Specifically, structures for **1c** with the C_3 and C_2 symmetries seen in **1a** and **1e**, respectively, were investigated (Figure 2). The lowest energy conformation was again found to be the C_3 symmetry structure that contains three symmetry-related polymethylene chains with g–a$_4$–g conformations. This structure was 0.6 kcal/mol lower in energy than the relaxed molecular structure, whereas the C_2 symmetry structure similar to that of **1e** was about 3.5 kcal/mol higher in energy than the relaxed molecular structure. Again, the major factor controlling the energy differences in the structures was the interchain van der Waals interactions, which are more successfully avoided in the C_3 symmetry structure.

Even-Chain-Length Bicycles. Crystal structures have been obtained for compounds **1b**,[4g] **1d**,[4g] **1f**, **2d**,[10] and **2f**. These compounds crystallized as a series of related structures. Drawings of **2d**, **1f**, and **2f** are shown in Figure 3; ORTEP drawings of **1b,d** have been published.[4g] A summary of the diffraction data for **1f** and **2d,f** is given in Table IX; fractional coordinates and isotropic thermal parameters are given in Tables X–XII, and a summary of selected distances and angles is presented in Table XIII.

Table X. Fractional Coordinates and Isotropic Thermal Parameters for 1f

atom	*x*	*y*	*z*	*B*(eq), Å^2
Sn(1)	0.0287 (2)	0.1250 (2)	0.1768 (2)	7.1 (1)
Sn(2)	−0.7053 (2)	0.2418 (1)	0.0236 (2)	7.0 (1)
Cl(1)	0.1880 (6)	0.0760 (6)	0.2118 (6)	9.4 (5)
Cl(2)	−0.8370 (7)	0.3090 (7)	0.0556 (8)	11.2 (6)
C(1)	0.052 (3)	0.230 (3)	0.246 (3)	13 (3)
C(2)	−0.026 (4)	0.277 (2)	0.271 (3)	10 (2)
C(3)	−0.110 (3)	0.287 (3)	0.196 (2)	11 (3)
C(4)	−0.196 (3)	0.335 (2)	0.211 (3)	10 (2)
C(5)	−0.277 (3)	0.339 (3)	0.135 (3)	12 (3)
C(6)	−0.367 (3)	0.381 (2)	0.149 (2)	8 (2)
C(7)	−0.453 (2)	0.377 (2)	0.066 (2)	7 (2)
C(8)	−0.550 (3)	0.409 (2)	0.077 (3)	8 (2)
C(9)	−0.635 (2)	0.403 (3)	−0.011 (3)	9 (2)
C(10)	−0.658 (2)	0.330 (2)	−0.051 (3)	9 (2)
C(11)	−0.043 (2)	0.035 (2)	0.220 (2)	9 (2)
C(12)	−0.016 (3)	0.020 (4)	0.329 (4)	15 (4)
C(13)	−0.061 (7)	0.062 (6)	0.376 (3)	30 (8)
C(14)	−0.190 (6)	0.045 (7)	0.364 (9)	34 (8)
C(15)	−0.190 (8)	0.110 (7)	0.385 (6)	26 (8)
C(16)	−0.305 (3)	0.116 (2)	0.372 (3)	10 (2)
C(17)	−0.357 (3)	0.131 (3)	0.281 (3)	10 (2)
C(18)	−0.463 (3)	0.156 (2)	0.267 (2)	11 (3)
C(19)	−0.524 (3)	0.177 (2)	0.169 (3)	9 (2)
C(20)	−0.622 (3)	0.211 (2)	0.159 (2)	8 (2)
C(21)	−0.014 (2)	0.133 (2)	0.027 (2)	8 (2)
C(22)	−0.109 (2)	0.086 (2)	−0.022 (2)	7 (2)
C(23)	−0.202 (3)	0.122 (2)	−0.014 (2)	9 (2)
C(24)	−0.289 (3)	0.083 (3)	−0.061 (3)	10 (2)
C(25)	−0.379 (3)	0.122 (2)	−0.060 (2)	9 (2)
C(26)	−0.474 (3)	0.078 (2)	−0.110 (2)	10 (2)
C(27)	−0.578 (3)	0.120 (2)	−0.096 (3)	13 (3)
C(28)	−0.660 (6)	0.086 (3)	−0.148 (4)	20 (5)
C(29)	−0.747 (3)	0.136 (2)	−0.152 (4)	12 (3)
C(30)	−0.772 (3)	0.151 (3)	−0.054 (3)	12 (3)

The two phenyl-substituted macrobicycles, **2d,f**, crystallized in the space group $C2/c$ as closely related homologous structures, although **2d** was disordered. Each

Table XI. Fractional Coordinates and Isotropic Thermal Parameters for 2d

atom	*x*	*y*	*z*	*U*(eq), Å^2
Sn	0.3985 (1)	0.2415 (1)	0.4746 (1)	0.113 (1)
C(1)	0.3765 (7)	0.0410 (16)	0.5195 (9)	0.131 (5)
C(2)	0.3165 (8)	0.0421 (18)	0.5217 (10)	0.151 (6)
C(3)	0.3221 (7)	0.1413 (18)	0.5931 (8)	0.099 (8)
C(3′)	0.3151 (12)	0.0206 (28)	0.6030 (9)	0.130 (29)
C(4)	0.3743 (6)	0.0865 (17)	0.6850 (8)	0.130 (5)
C(5)	0.6190 (7)	0.1952 (18)	0.7248 (9)	0.142 (5)
C(6)	0.5545 (7)	0.1655 (16)	0.6567 (9)	0.111 (7)
C(6′)	0.5961 (11)	0.1430 (28)	0.6504 (9)	0.061 (26)
C(7)	0.5510 (9)	0.2610 (17)	0.5855 (11)	0.161 (6)
C(8)	0.4931 (9)	0.2229 (16)	0.4977 (12)	0.141 (5)
C(9)	0.3850 (6)	0.4485 (16)	0.5172 (8)	0.130 (5)
C(10)	0.4349 (7)	0.4890 (15)	0.6132 (9)	0.094 (8)
C(10′)	0.4362 (13)	0.5676 (24)	0.5653 (15)	0.161 (29)
C(11)	0.4253 (7)	0.6501 (14)	0.6284 (10)	0.130 (5)
C(12)	0.4639 (8)	0.6609 (19)	0.7295 (12)	0.162 (7)
C(13)	0.2903 (8)	0.1450 (17)	0.2876 (10)	0.128 (11)
C(14)	0.2528 (7)	0.1459 (21)	0.2008 (11)	0.142 (11)
C(15)	0.2590 (7)	0.2446 (22)	0.1525 (10)	0.130 (10)
C(16)	0.3038 (9)	0.3478 (19)	0.1946 (11)	0.125 (11)
C(17)	0.3430 (6)	0.3479 (17)	0.2847 (11)	0.119 (11)
C(18)	0.3373 (6)	0.2451 (17)	0.3349 (8)	0.100 (7)

Table XII. Fractional Coordinates and Isotropic Thermal Parameters for 2f

atom	*x*	*y*	*z*	*B*(eq), Å^2
Sn	0.69313 (8)	0.0226 (2)	0.04464 (8)	8.83 (9)
C(1)	0.755 (1)	0.025 (3)	0.163 (1)	8 (1)
C(2)	0.754 (1)	0.124 (3)	0.212 (2)	10 (1)
C(3)	0.794 (2)	0.120 (3)	0.289 (2)	12 (2)
C(4)	0.838 (1)	0.021 (4)	0.317 (2)	11 (2)
C(5)	0.843 (1)	−0.076 (3)	0.272 (2)	11 (2)
C(6)	0.802 (2)	−0.070 (3)	0.197 (2)	11 (2)
C(7)	0.646 (1)	−0.175 (3)	0.020 (2)	12 (2)
C(8)	0.605 (2)	−0.212 (3)	−0.059 (2)	14 (2)
C(9)	0.570 (1)	−0.352 (4)	−0.078 (2)	14 (2)
C(10)	0.521 (2)	−0.366 (4)	−0.163 (3)	19 (3)
C(11)	0.530 (4)	−0.413 (7)	−0.207 (3)	27 (5)
C(12)	0.637 (1)	0.207 (3)	0.014 (1)	11 (2)
C(13)	0.586 (1)	0.202 (5)	0.027 (2)	17 (2)
C(14)	0.532 (2)	0.187 (6)	−0.018 (2)	24 (3)
C(15)	0.499 (1)	0.215 (4)	−0.101 (2)	16 (2)
C(16)	0.447 (1)	0.118 (3)	−0.148 (2)	12 (2)
C(17)	0.750 (1)	0.025 (3)	−0.000 (1)	12 (1)
C(18)	0.719 (1)	−0.003 (3)	−0.084 (1)	11 (1)
C(19)	0.666 (1)	0.082 (3)	−0.137 (1)	11 (1)
C(20)	0.638 (1)	0.052 (3)	−0.219 (1)	10 (1)
C(21)	0.585 (1)	0.146 (3)	−0.271 (2)	11 (1)

Table XIII. Selected Interatomic Distances and Angles for 1f, 2d, and 2f

Interatomic Distances (Å) in **1f**			
Sn(1)–Sn(2)	10.336 (4)	Sn(1)–Cl(1)	2.353 (8)
Sn(2)–Cl(2)	2.38 (1)	Sn(1)–C(1)	2.05 (5)
Sn(1)–C(11)	2.05 (4)	Sn(1)–C(21)	2.18 (3)
Sn(2)–C(10)	2.11 (4)	Sn(2)–C(20)	2.12 (3)
Sn(2)–C(30)	2.01 (5)		
Bond Angles (deg) in **1f**			
Cl(1)–Sn(1)–C(1)	101 (1)	Cl(1)–Sn(1)–C(11)	102 (1)
Cl(1)–Sn(1)–C(21)	103 (1)	Cl(2)–Sn(2)–C(10)	99 (1)
Cl(2)–Sn(2)–C(20)	101 (1)	Cl(2)–Sn(2)–C(30)	102 (1)
C(1)–Sn(1)–C(11)	121 (1)	C(1)–Sn(1)–C(21)	116 (2)
C(11)–Sn(1)–C(21)	111 (1)	C(10)–Sn(2)–C(20)	121 (1)
C(10)–Sn(2)–C(30)	114 (2)	C(20)–Sn(2)–C(30)	115 (1)
Interatomic Distances (Å) in **2d**			
Sn–C(1)	2.206 (18)	Sn–C(8)	2.209 (23)
Sn–C(9)	2.145 (16)	Sn–C(18)	2.142 (12)
C(1)–C(2)	1.551 (31)	C(2)–C(3)	1.540 (25)
C(2)–C(3′)	1.540 (33)	C(3)–C(3′)	1.146 (31)
C(3)–C(4)	1.540 (16)	C(3′)–C(4)	1.540 (22)
C(5)–C(6)	1.540 (16)	C(5)–C(6′)	1.540 (25)
C(6)–C(6′)	1.149 (36)	C(6)–C(7)	1.540 (27)
C(6′)–C(7)	1.540 (26)	C(7)–C(8)	1.499 (20)
C(9)–C(10)	1.540 (16)	C(9)–C(10′)	1.540 (27)
C(10)–C(10′)	1.155 (35)	C(10)–C(11)	1.540 (20)
C(10′)–C(11)	1.540 (39)	C(11)–C(12)	1.552 (25)
Sn–Sn(a)	8.453 (1)		
Bond Angles (deg) in **2d**			
C(1)–Sn–C(8)	110.2 (6)	C(1)–Sn–C(9)	117.5 (7)
C(8)–Sn–C(9)	112.3 (6)	C(1)–Sn–C(18)	107.4 (5)
C(8)–Sn–C(18)	102.2 (7)	C(9)–Sn–C(18)	105.8 (5)
Sn–C(1)–C(2)	117.9 (10)	Sn–C(8)–C(7)	119.8 (17)
Sn–C(9)–C(10)	115.8 (9)	Sn–C(9)–C(10′)	125.0 (16)
Interatomic Distances (Å) in **2f**			
Sn–Sn	11.055 (6)	Sn–C(1)	2.13 (2)
Sn–C(7)	2.09 (3)	Sn–C(12)	2.10 (3)
Sn–C(17)	2.14 (2)		
Bond Angles (deg) in **2f**			
C(1)–Sn–C(7)	106 (1)	C(1)–Sn–C(12)	108 (1)
C(1)–Sn–C(17)	105 (1)	C(7)–Sn–C(12)	114.0 (9)
C(7)–Sn–C(17)	110 (1)	C(12)–Sn–C(17)	112.8 (8)

Table XIV. Comparison of Calculated and Experimental Structures for 2f

	MM2	exptl[a]
Interatomic Distances (Å)		
Sn–Sn	11.382	11.055 (6)
Sn–C(1)	2.151	2.13 (2)
Sn–C(7)	2.151	2.09 (3)
Sn–C(12)	2.151	2.10 (3)
Sn–C(17)	2.151	2.14 (2)
Bond Angles (deg)		
C(1)–Sn–C(7)	106.0	106 (1)
C(1)–Sn–C(12)	108.6	108 (1)
C(1)–Sn–C(17)	106.6	105 (1)
C(7)–Sn–C(12)	115.9	114.0 (9)
C(7)–Sn–C(17)	112.5	110 (1)
C(12)–Sn–C(17)	106.8	112.8 (8)
Torsion Angles (deg)		
Sn–C(7)–C(8)–C(9)	−176.5	−180 (2)
Sn–C(12)–C(13)–C(14)	−72.5	−105 (6)
Sn–C(17)–C(18)–C(19)	59.6	52 (3)

[a] X-ray crystal structure, this work.

molecule contained a single C_2 axis that is perpendicular to the tin–tin axis and passes through the center of one of the chains. The drawings of these compounds in Figure 3 show views down the C_2 axis of each molecule. In both of these compounds, the two symmetry-related chains adopted highly regular conformations with the gauche interactions at the ends of the chains (g_2–a_{n-4}–g) and the chains running antiparallel to one another; this conformation apparently successfully minimizes interchain interactions. For both compounds, we did not find conformations at energy lower than that of the relaxed molecular structures in MM2 modeling, although the arrangement of chains seen in compound **1d** (see below) gave a structure only slightly higher in energy than the relaxed molecular structure. For both **2d** and **2f**, the MM2 minimized structures resulted in Sn–Sn distances that were significantly greater than those in the crystals. Because most of the bond angles involving tin in both structures were accurately reproduced, the origin for these differences appears to be an extension of the polymethylene chains in the calculated structures. Comparisons of experimental and calculated structural features for **2f** and **2d**, respectively, are given in Table XIV and Table XVIII (supplementary material).

The C-8 bicyclic chloride (**1d**) also crystallized in the space group *C*2/*c* with a C_2 axis passing through the center of one of the chains.[4g] However, the conformations adopted by the chains in **1d** were different from those seen above. Wheras **2d** contained two chains with g_2–a_4–g

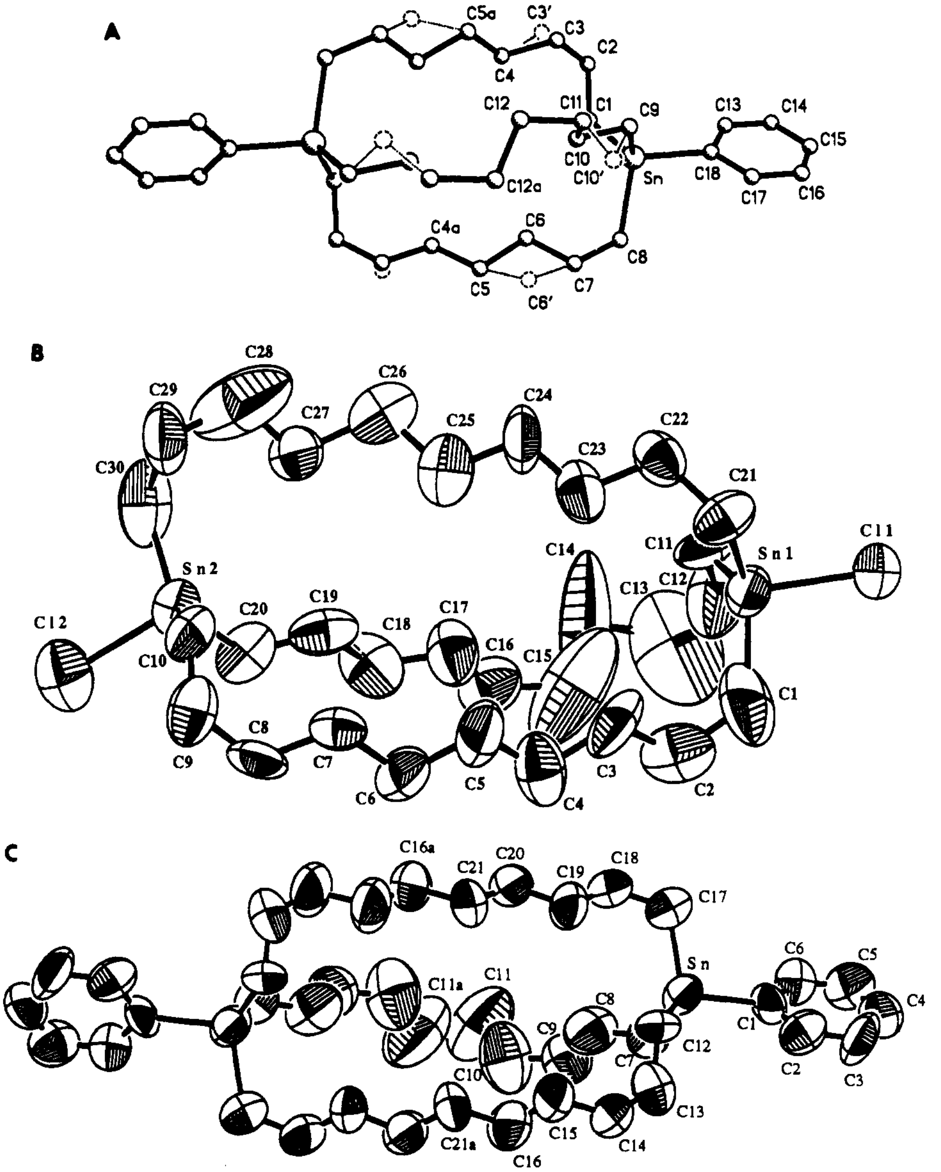

Figure 3. Drawings of structures of **2d** (A), **1f** (B), and **2f** (C). The ball and stick drawing of **2d** shows the disorder in the crystal. The ORTEP drawings of **1f** and **2f** are at 50% probability.

conformations, **1d** contained two chains with a_2–g_3–a–g conformations (Figure 4). MM2 modeling indicated that for **1d** there was essentially no energy difference between these two possible C_2 symmetry structures. Table XV contains a comparison of the calculated and experimental features. Unlike the case with compounds **2d**,**f** discussed above, the calculated Sn–Sn distance in **1d** closely matched the experimental value. Apparently, the chain conformation found in **1d** does not permit a low-energy "extension" of the polymethylene chains.

Table XV. Comparison of Calculated and Experimental Structures for 1d

	MM2	expt1[a]
Interatomic Distances (Å)		
Sn–Sn	7.545	7.566 (2)
Sn–Cl	2.379	2.373 (3)
Sn–C(1)	2.145	2.12 (1)
Sn–C(5)	2.145	2.08 (2)
Sn–C(12)	2.148	2.11 (1)
Bond Angles (deg)		
Cl–Sn–C(1)	102.8	99.4 (4)
Cl–Sn–C(5)	102.4	101.1 (4)
Cl–Sn–C(9)	103.8	104.6 (3)
C(1)–Sn–C(5)	114.5	115.8 (5)
C(1)–Sn–C(9)	117.0	115.5 (5)
C(5)–Sn–C(9)	113.7	116.6 (5)

[a] X-ray crystal structure, ref 4g.

The C-10 bicyclic chloride (**1f**) crystallized in a conformation similar to those of the diphenyl-substituted members of this group. Two chains adopted the g_2–a_6–g conformation, but these conformations ran parallel rather than antiparallel to one another, and thus the molecule did not contain a C_2 axis. Table XIX (supplementary material) contains features for the crystal structure and MM2 relaxed molecular structure (Figure 4) of **1f**. The agreement between experimental and calculated bond angles involving tin was extremely good. A structure for **1f** with true C_2 symmetry and a C_3 symmetry structure (Figure 4) also were modeled. The C_2 symmetry structure was found to be the lowest energy structure, and the C_3 symmetry structure was intermediate in energy between the C_2 structure and the relaxed molecular structure.

The crystal structure of the small C-6 bicyclic chloride (**1b**)[4g] lacked a C_2 axis but actually was quite similar to the structures of **2d**,**f** discussed above. Two polymethylene chains in **1b** had nearly identical conformations and appeared to be related to one another by a C_2 axis, but the

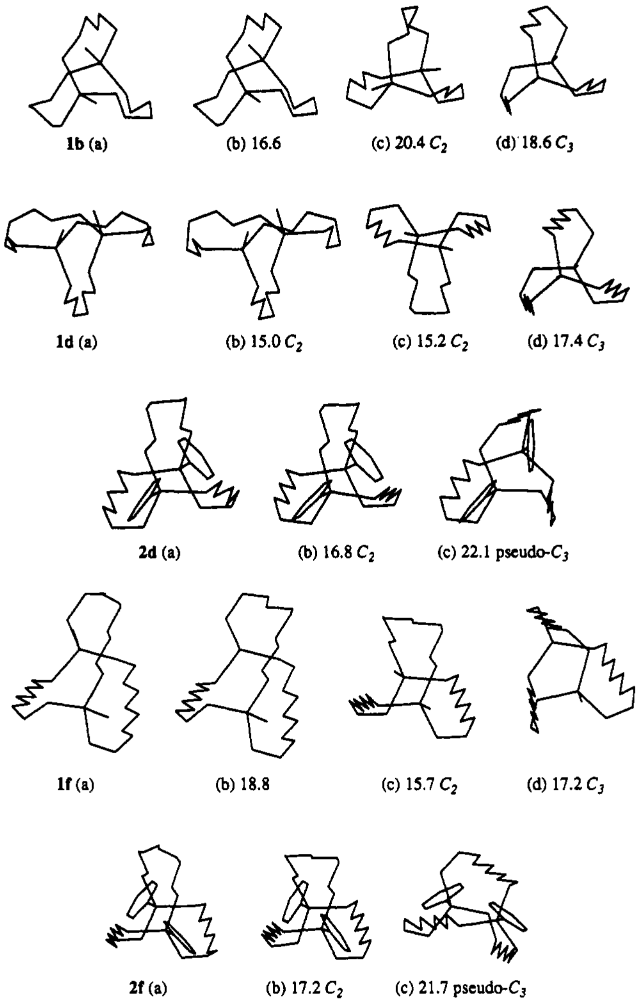

1b (a) (b) 16.6 (c) 20.4 C_2 (d) 18.6 C_3

1d (a) (b) 15.0 C_2 (c) 15.2 C_2 (d) 17.4 C_3

2d (a) (b) 16.8 C_2 (c) 22.1 pseudo-C_3

1f (a) (b) 18.8 (c) 15.7 C_2 (d) 17.2 C_3

2f (a) (b) 17.2 C_2 (c) 21.7 pseudo-C_3

Figure 4. Even-chain-length macrobicycles. See caption to Figure 2.

symmetry element was absent in **1b** because the halves of the third chain, through which the C_2 axis should run, were not equivalent. The comparison of the MM2 minimized relaxed molecular structure and actual structure of compound **1b** (Figure 4) is contained in Table XX (supplementary material). The Sn–Sn distance was closely approximated in the calculations, but distances and angles around tin were poorly modeled. It should be noted, however, that the crystal structure of **1b** contained a number of nonstandard distances and angles involving tin. For example, values for the Sn–C bond distances ranged from 2.01 to 2.26 Å, and values for C–Sn–C bond angles ranged from 106 to 125°.[4g] The most plausible explanation for these unusual values is disorder or high thermal motion in the crystal, but no attempt was made to resolve this disorder.[4g]

The energies of various possible structures for **1b** were calculated. These included the relaxed molecular structure, a structure with true C_2 symmetry wherein the symmetry-related chains have g_2–a_2–g conformations and a structure with C_3 symmetry (Figure 4). The relaxed molecular structure was found to be the lowest in energy; the C_3 structure was 2 kcal/mol higher in energy, and the C_2 structure was almost 4 kcal/mol higher in energy.

For the odd-chain-length macrobicycles described earlier, the minimum-enegy conformation found was that with C_3 symmetry with the axis running through the two tin atoms, but no such structures were observed for the even-chain-length compounds. However, we could readily test the energies of C_3 symmetry structures for the even-chain-length members by MM2 modeling (Figure 4). Each structure contained the three chains in a g_2–a_{n-4}–g conformation running parallel to one another. Except for the small bicycle **1b**, the C_3 symmetry structure was about 2 kcal/mol higher in energy than the typically observed C_2 symmetry structures with two g_2–a_{n-4}–g conformation chains running antiparallel.

Modeling Conclusions

Although MM2 modeling cannot account for crystal-packing forces, the generally good agreement between the observed structures of the macrobicycles and the calculated minimum-energy conformations is gratifying. The MM2 calculations of relaxed molecular structures and the actual crystal structures often agreed quite well. Generally, the greatest discrepancies between the two were found to occur at positions of high thermal motion or disorder in the crystal; these discrepancies most often were manifested as calculated Sn–C bond lengths that were typical in comparison to other compounds but longer than those observed in the specific crystal structure. Such behavior is not unexpected because high thermal motion of atom X relative to atom Y will result in an apparent X–Y bond length that is too short.[11] For some simple structural features such as the transannular Sn–Sn distance, the MM2 minimum-energy structure usually resulted in a good approximation even when it was not the observed structure in the solid state.

We consider the observed marked differences between the structures of the members of the odd- and even-chain series of macrobicycles to be an especially important feature that the modeling predicted well, and we consider it quite likely that this structural difference will also be present for the bicycles in solution. For less rigid systems such as simple macrocycles, where crystal-packing forces might be substantially more important in controlling the solid-state structures, it is likely that the MM2 calculated minima, rather than the crystal structures, will better represent the structures in solution. The tetrahedral tin parameters developed in the accompanying paper were shown to be adequate for modeling several small stannanes,[8] and this work has shown that MM2 modeling of large tin-containing compounds can also be useful.

Experimental Section

Materials. The preparations of **1c,f** and **2d,f** have been reported.[4f] The melting points (uncorrected) and recrystallization solvents for the crystal samples were as follows: **1c**, mp 138–139 °C from chloroform–hexane; **1f**, mp 30–35 °C from hexane; **2d**, mp 92–94 °C from THF–methanol; **2f**, mp 56–58 °C from THF–methanol. Polymorphism is possible for **1f**; a sample of this compound with mp 88–90 °C has been obtained. Compounds **1a**, **2a**, and **1e** are new; they were prepared by schemes similar to those reported.[4f]

1,7-Dichloro-1,7-distannabicyclo[5.5.5]heptadecane (1a) was recrystallized from acetonitrile: mp 153–155 °C; ^{13}C NMR (CDCl$_3$, 50 MHz, internal Me$_4$Si) δ 38.5, 26.2, 21.0; ^{119}Sn NMR (CDCl$_3$, 149 MHz, internal Me$_4$Sn) δ 171.6.

1,7-Diphenyl-1,7-distannabicyclo[5.5.5]heptadecane (2a) was recrystallized from THF–methanol: mp 165–168 °C; ^{13}C NMR (CDCl$_3$, 50 MHz, internal Me$_4$Si) δ 144.8, 135.7, 127.8 (2 unresolved lines), 37.4, 26.7, 11.7.

1,11-Dichloro-1,11-distannabicyclo[9.9.9]nonacosane (1e) was recrystallized from hexane: mp 114–116 °C; ^{13}C NMR (CDCl$_3$, 50 MHz, internal Me$_4$Si) δ 33.96, 29.23, 28.94, 25.78, 19.30; ^{119}Sn NMR (CDCl$_3$, 149 MHz, internal Me$_4$Sn) δ 151.0.

Computations. Modeling calculations were performed as described in the accompanying paper.[8]

---

(11) Schomaker, V.; Trueblood, K. N. *Acta Crystallogr., Sect. B* **1968**, *B24*, 63.

Crystallographic Analyses of 1a,c,e,f and 2a,f. General Considerations. Suitable crystals of **1a,c,e,f** and **2a,f**, mounted on glass fibers with silicone cement, were examined at room temperature on a Rigaku AFC5R four-circle diffractometer equipped with a 12-kW rotating-anode Mo X-ray source (graphite monochromated Kα, $\lambda = 0.71069$ Å). Unit cells were refined from 25 randomly selected reflections obtained by the AFC5R search and index routines. For **1a,c,f** and **2a**, the unit cell parameters were more precisely refined by using up to 25 additional high-angle reflections. No high-angle unit cell was obtained for **1e** or **2f** due to the lack of suitably intense reflections at high 2θ angles. Structure solutions and refinements were performed on a Digital Equipment Corp. MicroVAX II computer with the TEXSAN series of programs.[12] During data collection, weak reflections were scanned up to three times. The intensities of three standard reflections, observed at 150 reflection intervals throughout data collection, were monitored for decay, and decay corrections were applied when required. Where necessary, an empirical absorption correction based on ψ scans was applied; normalized transmission factors are included in the summary tables. Except for compound **1c**, the tin atoms were found on *E* maps calculated by the program MITHRIL.[13] In the case of **1c**, the tin atoms were located from a Patterson map. In all cases, the carbon and chlorine atoms were located on successive electron density maps calculated by using direct-method phase refinement techniques (DIRDIF).[14] In all cases except **2a**, the hydrogens were placed in ideal positions ($d_{C-H} = 0.95$ Å) and were included in subsequent refinements as fixed isotropic scatterers. In the case of **2a**, difference electron maps revealed the positions of all hydrogen atoms, which were then included in subsequent refinements as fixed isotropic scatterers. All structures were refined by full-matrix least squares with anisotropic thermal parameters for all non-hydrogen atoms; the function minimized was $\sum w(|F_o| - |F_c|)^2$, where $w = (\sigma^2(F_o))^{-1}$. Intense reflections were downweighted with use of a factor of $p = 0.05$.[12,15] Except for **2f**, the final refinements were performed on those data for which $I > 3\sigma(I)$; the final refinement was performed on those data for which $I > 2\sigma(I)$ for **2f**. In each case an analysis of F_o versus F_c as a function of $(\sin\theta)/\lambda$, Miller indices, and F_o displayed no unusual trends. The final difference Fourier maps contained no significant residual electron density. Crystal data, data collection parameters, and results of analyses are given in Tables I and IX.

It should be noted that positional disorder within the bridging chains increased as the chains became longer. For **1c,e,f** and **2f**, the disorder appeared to be confined primarily to a single chain: C(15) to C(21) for **1c**, C(1) to C(1a) for **1e**, C(12) to C(15) for **1f**, and C(7) to C(7a) for **2f**. Attempts to resolve the disorder in **1c** were unsuccessful. Disorder was successfully resolved for **2d** (see below).

Compound 1a. Intensity statistics strongly indicated a centrosymmetric space group, which with the systematic absence ($00l$, $l \neq 2n$) indicated the space group $P6_3/m$. The reflections for which $h - k = 3$ and $l \neq 2n$ were systematically much weaker than those for which $h - k = 3n$ and $l = 2n$, which is consistent with the tin and chlorine atoms being present on the special positions $^2/_3$, $^1/_3$, z. Because the data set for **1a** contained a disproportionately large number of intense reflections, the use of a p factor of 0.05 resulted in an underestimation of σ for the intense reflections and an unrealistically low value for the GOF of 0.87.[15] When the p factor was reduced to 0.03, a more satisfactory GOF of 1.05 was obtained.

Compound 1c. The space group was assigned as $P2_1/n$ on the basis of intensity statistics and systematic absences ($h0l$, $h + l \neq 2n$; $0k0$, $k \neq 2n$).

Compound 1e. Systematic absences (hkl, $h + k \neq 2n$; $h0l$, $l \neq 2n$) indicated either space group $C2/c$ or Cc. The structure was originally solved in space group, Cc, but a number of highly irregular bond distances and the presence of an inversion center indicated that this was not correct. A much more satisfactory solution was then obtained in the centrosymmetric space group $C2/c$.

Compounds 1f and 2a. The space group was assigned as $P2_1/c$ on the basis of intensity statistics and systematic absences ($0k0$, $l \neq 2n$; $h0l$, $l \neq 2n$).

Compound 2f. The space group was assigned as $C2/c$ on the basis of systematic absences (hkl, $l \neq 2n$; $h0l$, $l \neq 2n$) and intensity statistics.

Crystallographic Analysis of 2d. A colorless parallelepiped was mounted on a glass fiber with epoxy cement. Preliminary examination and data collection were performed on a Nicolet R3m X-ray diffractometer. Cell parameters were calculated from the least-squares fitting of the setting angles for 25 reflections. ω scans for several intense reflections indicated acceptable crystal quality. Three control reflections collected every 97 reflections showed no significant trends. Lorentz and polarization corrections were applied. No absorption correction was applied. Reflections intensities were profiled by employing a learned profile technique.[16] The space group was assigned as $C2/c$ on the basis of systematic absences (hkl, $l \neq 2n$; $h0l$, $l \neq 2n$) and intensity statistics.

The structure was solved by direct methods with use of the SHELXTL-PLUS program package.[17] The structure was initially refined to convergence with use of full-matrix anisotropic least-squares refinement for all non-hydrogen atoms. Large distorted thermal ellipsoids for C(3), C(6), and C(10) and nonstandard bond lengths involving these atoms indicated disorder at these positions. Consequently, the distances between the following pairs of atoms were constrained to 1.540 (1) Å: C(2), C(3); C(3), C(4); C(5), C(6); C(6), C(7); C(9), C(10); C(10), C(11). With these constraints applied, positions for C(3′), C(6′), and C(10′) were located from subsequent Fourier difference maps, and the distances involving these sites were then constrained as above. Site occupation factors were refined together for the following atom pairs: C(3), C(3′); C(6), C(6′); C(10), C(10′). The resulting site occupation factors (C(3) 75%, C(3′) 25%; C(6) 84%, C(6′) 16%, C(10) 70%, C(10′) 30%) were used in the final stages of refinement, and the model was refined to convergence. In the final structure, the atoms Sn, C(13), C(14), C(15), C(16), C(17), and C(18) were refined by full-matrix anisotropic least-squares analysis. The remaining non-hydrogen atoms were refined isotropically. Hydrogen atoms were placed in idealized positions with isotropic thermal parameters fixed at 0.08 Å^2. Neutral-atom scattering factors and anomalous scattering correction terms were taken from literature values.[18] Structure factor weights were calculated with $w = (\sigma^2(F) + gF^2)^{-1}$, where $g = 1 \times 10^{-5}$.

Acknowledgment. We thank the Office of Naval Research for financial support. P.J.S. acknowledges support from the Robert A. Welch Foundation. The Rigaku AFC5R diffractometer was obtained under DOD Contract No. N-00014-86-G-0194. The Nicolet R3m/V diffractometer and computing system was purchased with funds provided by the National Science Foundation (Grant No. CHE-8513273).

Supplementary Material Available: Tables of positional parameters for all atoms and anisotropic thermal parameters for the non-hydrogen atoms for **1a,c,e,f** and **2a,d,f**, complete listings of bond distances and bond angles for **1c,e,f** and **2a,d,f**, and Tables XVI–XX, containing comparisons of experimental and MM2 calculated structural features for **2a**, **1c**, **2d**, **1f**, and **1b** (44 pages); listings of observed and calculated structure factors for **1c,e,f** and **2a,d,f** (147 pages). Ordering information is given on any current masthead page.

---

(12) TEXSAN, *Texray Structural Analysis Package*; Molecular Structure Corp.: The Woodlands, TX, 1987; revised.

(13) Gilmore, C. J. MITHRIL: *A Computer Program for the Automatic Solution of Crystal Structures from X-ray Data*; University of Glasgow: Glasgow, Scotland, 1983.

(14) Beurskens, P. T. DIRDIF: *Direct Methods for Difference Structures—An Automatic Procedure for Phase Extension and Refinement of Difference Structure Factors*; Technical Report 1984/1; Crystallography Laboratory: Toernooiveld, The Netherlands.

(15) Doedens, R. J.; Ibers, J. A. *Inorg. Chem.* **1967**, *6*, 204.

(16) Diamond, R. *Acta Crystallogr., Sect. A* **1969**, *A25*, 43.

(17) Sheldrick, B. M. SHELXTL PLUS program package, supplied by Nicolet XRD Corp.

(18) *International Tables for X-ray Crystallography*; Kynoch Press: Birmingham, England, 1974; Vol. IV.